

Shewhart control schemes with supplementary 2-of-(h+1) side-sensitive runs-rules under the Burr-type XII distribution

Jean-Claude Malela-Majika^{1,*}

P O Box 392 UNISA 0003, Pretoria

+27 (0) 11 670 9243

malelm@unisa.ac.za

Orcid ID: 0000-0001-7236-7678

Serge Kajingulu Malandala¹

P O Box 392 UNISA 0003, Pretoria

+27 (0) 11 670 9910

Email: malank@unisa.ac.za

Marien Alet Graham^c

Faculty of Education, University of Pretoria, Groenkloof Campus, Natural Sciences Building

Room 4-18, Corner of George Storrar Drive and Leyds Street, Groenkloof, Pretoria, 0002

+27 (0) 12 420 6637

Email: marien.graham@up.ac.za

Tel : +27 73 384 6103/ +27 11 670 9243. Fax: +27 12 429 8129.

¹*Department of Statistics, College of Science, Engineering and Technology, University of South Africa, P O Box 392 UNISA 0003, Pretoria, South Africa*

²*Department of Science, Mathematics & Technology Education, University of Pretoria, Pretoria, South Africa*

* Corresponding author. E-mail: malelm@unisa.ac.za

Highlights

- The manuscript presents closed-form of the characteristics of the run-length distribution of the $2\text{-of-}(h+1)$ runs-rules precedence schemes.
- The proposed side-sensitive $2\text{-of-}(h+1)$ schemes outperform significantly the non-side-sensitive schemes proposed by Malela-Majika et al. (2017).
- The proposed schemes are very efficient in detecting small to large shifts.
- They have very interesting zero-state and steady-state characteristics of the run-length under symmetric and skewed distributions.
- They outperform the traditional counterparts in many situations under normal and non-normal distributions.

Abstract

Control schemes that require strict distributional assumptions are called parametric control schemes. When the distributional assumptions fail to hold, nonparametric control schemes and other schemes based on more flexible probability distributions are needed. The traditional Shewhart control scheme has been improved upon using various techniques, one being the addition of non-side-sensitive (NSS) and side-sensitive runs-rules. Many authors showed that side-sensitive runs-rules schemes are significantly superior to NSS runs-rules schemes. In this paper, we propose side-sensitive Shewhart-type \bar{X} schemes supplemented with $2\text{-of-}(h+1)$ standard and improved runs-rules (where h is a non-zero positive integer) under the violation of the normality assumption for monitoring the process mean. The zero-state and steady-state performances of the proposed schemes are investigated using a Markov chain approach. It is observed that the proposed schemes outperform the existing schemes in many situations and possess very interesting zero-state and steady-state properties under normal and non-normal distributions. An illustrative example is provided to facilitate the design and implementation of the proposed schemes.

Keywords: side-sensitive schemes; runs-rules; Markov chain approach; zero-state performance; steady-state performance

1. Introduction

A control chart is one of the most powerful tools used in statistical process control and monitoring (SPCM). Control charts help to identify two sources of variations in the quality process, namely common (or chance) causes and special (or assignable) causes of variation. Chance causes are expected in any process. A process that runs in the presence of chance causes without showing any pattern is said to be in-control (IC). On the other hand, a process that runs in the presence of assignable causes is said to be out-of-control (OOC), which means that there is a problem in the process, which must be found and eliminated. Under normally distributed data, researchers advocate the use of parametric control charts because of their simplicity in the design; implementation and computation of the characteristics of the run-length distribution (cf. Montgomery¹). However, one of the drawbacks of parametric (or classical) control charts is that they are not IC robust and they are relatively inefficient under the violation of the normality assumption (cf. Chakraborti et al²). To overcome this limitation, we need either nonparametric or flexible control charts, which do not rely on parametric assumptions (cf. Malela-Majika et al³). Recently, Guo and Wang⁴ proposed control charts for monitoring the Weibull shape parameter when the sample is type-II censored. Chen⁵ suggested a Shewhart-type scheme for monitoring both shape and scale parameters of Weibull data without subgrouping. Azam et al⁶ developed an \bar{X} chart for Burr-type XII distribution under repetitive sampling. The comparison of different control charts for a Weibull process with type-I censoring was presented by Bizuneh and Wang.⁷ The simplest and most basic scheme of these charts is denoted 1-of-1 (or RR_{1-of-1}) scheme. This chart gives a signal if the sample mean (i.e. \bar{X}) plots beyond the control limits given in equation by

$$UCL / LCL = \mu_0 \pm k \sigma_0, \quad (1)$$

where k is the distance of the control limits from the centerline, UCL and LCL represent the upper and lower control limits of the basic scheme, respectively (see Figure 1 (a)).

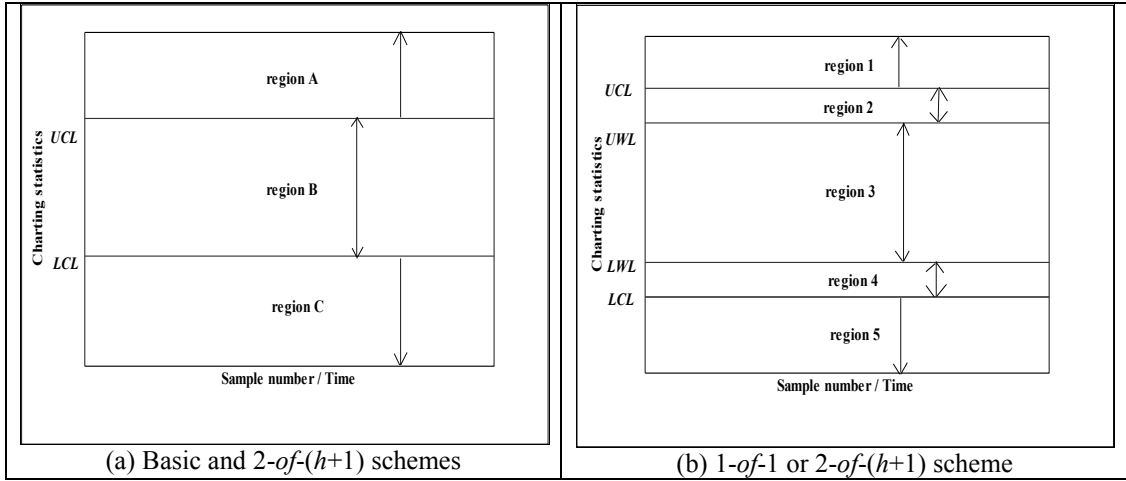


Figure 1. \bar{X} Burr XII control schemes regions

To improve the sensitivity of the basic scheme for detecting small to moderate shifts in process parameter(s), researchers have proposed different techniques which include the introduction of addition limits, referred to as warning limits (WL), which are typically used in conjunction with the addition of runs-rules (see, for example, Champ and Woodall⁸). Other techniques such as adaptive features have also been considered in the literature (see, for example, Reynolds et al⁹), however, these are not considered in this study; the focus here is supplementary runs-rules.

In the case where warning limits and runs-rules are introduced (see Figure 1(b)), the control limits and warning limits are given by

$$UWL / LWL = \mu_0 \pm k_1 \sigma_0$$

and

$$UCL / LCL = \mu_0 \pm k_2 \sigma_0,$$
(2)

respectively; where k_1 and k_2 denote the distance of the warning and control limits from the centerline (CL) in standard deviation units, respectively, with $k_2 > k_1 > 0$. Now, both k_1 and k_2 need to be determined so that the charts meet some specified performance criterion, e.g., a pre-specified value for the IC average run-length (ARL_0).

Khoo¹⁰ proposed the m -of- k standard runs-rules (hereafter SRR_{m-of-k}) schemes (where $(m, k) = (2, 4), (3, 3)$ and $(3, 4)$) using a Markov chain approach. The SRR_{m-of-k} scheme signals when m out of k ($m > 1$ and $k \geq m$) consecutive samples plot beyond the control limits given in Figure 1 (a). The SRR_{m-of-k} scheme increases the performance of the basic scheme in detecting small and moderate shifts. However, the basic Shewhart-type scheme outperforms the SRR_{m-of-k} scheme in detecting large shifts in the process. Khoo and Ariffin¹¹ and Acosta-Mejia¹²

improved Khoo¹⁰'s runs-rules schemes in detecting large mean shifts by combining the basic and SRR_{m-of-k} schemes. The improved scheme is called improved runs-rules (IRR) denoted by IRR_{m-of-k} . This scheme gives a signal when either one sample falls beyond the control limits (in region 1 or 5) or when m out of k consecutive samples plot between the warning and control limits, no matter whether some (or all) of the m samples fall in region 2 and others (or all) fall in region 4 (see Figure 1(b)). Champ and Woodall⁸ and Koutras et al¹³ investigated the average run-length performance (ARL) of the Shewhart-type chart with supplementary runs-rules using the Markov chain approach. A number of authors including Champ and Woodall⁸ and Davis and Woodall¹⁴ showed that runs-rules and particularly Western electric sensitising rules can improve the sensitivity of the control scheme to detect small shifts and considerably increase the ARL_0 . However, these rules can considerably increase the false alarm rate (FAR) (cf Montgomery,¹ pages 198 and 199). Shongwe and Graham^{15, 16} proposed Shewhart-type \bar{X} charts using a variety of synthetic and runs-rules schemes. Using the approach discussed in Shongwe and Graham,¹⁵ Malela-Majika et al³ proposed the non-side-sensitive (NSS) 2-*of*-($h+1$) SRR and IRR control schemes using the Burr-type XII (BTXII) distribution for monitoring the process mean for non-normal data. Mehmood et al¹⁷ investigated the performance of the \bar{X} control chart for known and unknown parameters supplemented with runs-rules under different probability distributions. Tran¹⁸ designed the t chart with supplementary runs-rules for monitoring changes in the location process parameter. In this paper, we propose the side-sensitive $SRR_{2-of-(h+1)}$ and $IRR_{2-of-(h+1)}$ schemes when the assumption of normality fails to hold. The zero-state and steady-state ARL and average extra quadratic loss ($AEQL$) performance measures are thoroughly investigated using the Markov chain approach.

This paper uses the side-sensitive 2-*of*-($h+1$) and 1-*of*-1 or 2-*of*-($h+1$) schemes to expand the Shewhart-type \bar{X} scheme for non-normal distributed data under the assumption of known process parameters (Case K) for monitoring the process mean. The zero-state (ZS) and steady-state (SS) performances are investigated using the Markov chain approach. The proposed schemes with unknown process parameter (Case U) is under investigation and will be soon reported in a separate article.

The remainder of this paper is presented as follows: Section 2 introduces the design of the side-sensitive 2-*of*-($h+1$) and 1-*of*-1 or 2-*of*-($h+1$) Shewhart \bar{X} schemes using the BTXII distribution. In Section 3, the ZS and SS characteristics of the run-length distribution of the proposed side-sensitive schemes are derived using the Markov chain approach. In Section 4, the IC and OOC

performances of the proposed schemes are discussed and compared to the NSS 2-*of*-($h+1$) and 1-*of*-1 or 2-*of*-($h+1$) Shewhart-type \bar{X} schemes for normal and non-normal data. An illustrative example is given in Section 5 using real-life data to demonstrate the design and implementation of the proposed side-sensitive schemes. Concluding remarks and some recommendations are given in Section 6.

2. Design of the proposed Shewhart \bar{X} schemes under the BTXII distribution

The BTXII distribution is used to describe the non-normal probability density function of the IC process (cf Burr¹⁹). The advantages of this distribution include the simplicity of its cumulative distribution function (cdf) (see Equation (3)) as well as the possibility of representing several different unimodal distributions. Consequently, the calculations of the type I and type II errors as well as the closed-form of the run-length distribution of control charts designed under the BTXII distribution are easier to obtain.

Assume that $\{X_{ij}; i \geq 1 \text{ and } j = 1, \dots, n\}$ is a sequence of independent and identically distributed (iid) samples from a $N(\mu_0, \sigma_0^2)$ distribution with IC process mean μ_0 and IC process standard deviation σ_0 . The cdf of the BTXII distribution is given by

$$F(y) = 1 - \frac{1}{(1+y^c)^q} \text{ for } y \geq 0, \quad (3)$$

where c and q are greater than one and represent the skewness and kurtosis of the Burr distribution, respectively. Chen²⁰ showed that there is a relationship between a BTXII variable, Y , and any random variable X which is obtained through a standardised transformation where the skewness and kurtosis coefficients of the original sample are first estimated, and then these estimates are used to obtain the skewness and kurtosis of the BTXII distribution. Assuming that the random variables X and Y have the same skewness and kurtosis; therefore,

$$\frac{X-\bar{X}}{s_x} = \frac{Y-M}{S}, \quad (4)$$

where \bar{X} and s_x represent the sample mean and standard deviation of the data set, respectively, and M and S represent the mean and standard deviation of the corresponding BTXII distribution with different shapes.

From Equation (4), the sample mean can be defined by

$$\bar{X} = \mu_0 + (Y - M) \frac{\sigma_0}{S\sqrt{n}}, \quad (5)$$

Tables of the expected mean, standard deviation, skewness coefficient and kurtosis coefficient of the Burr distribution for various combinations of BTXII parameters c and q are presented in Burr.^{19, 21}

For a basic scheme, since the quality characteristic follows a BTXII distribution, the probability of accepting the process to be IC (i.e. a subgroup mean falling within the limits defined in Equation (1)) at the acceptable process level μ_0 , which is the probability that the process is IC, is given by

$$\beta = P(LCL \leq \bar{X} \leq UCL) = \frac{1}{[1 + (M - kS)^c]^q} - \frac{1}{[1 + (M + kS)^c]^q} \quad (6)$$

When the process mean has shifted to $\mu_1 = \mu_0 + \delta\sigma_0$ with $\delta \neq 0$, then the probability that the process is IC at the unacceptable level μ_1 (type II risk), β , which is the probability of no false alarms, defined by $P(LCL \leq \bar{X} \leq UCL | \mu = \mu_1)$, is given by

$$\beta = \frac{1}{[1 + (M - S(k - \delta\sqrt{n}))^c]^q} - \frac{1}{[1 + (M + S(k + \delta\sqrt{n}))^c]^q}, \quad (7)$$

where δ represents the change (or shift) in the location process parameter.

Therefore, the IC average run-length (ARL_0) of the basic Shewhart-type \bar{X} scheme under the BTXII distribution is given by

$$ARL_0 = \frac{1}{1 - \left(\frac{1}{[1 + (M - kS)^c]^q} - \frac{1}{[1 + (M + kS)^c]^q} \right)}, \quad (8)$$

and the OOC average run-length (ARL_δ) is given by

$$ARL_\delta = \frac{1}{1 - \left(\frac{1}{[1 + (M - S(k - \delta\sqrt{n}))^c]^q} - \frac{1}{[1 + (M + S(k + \delta\sqrt{n}))^c]^q} \right)}. \quad (9)$$

2.1 The side-sensitive $SRR_{2-of-(h+1)}$ and $IRR_{2-of-(h+1)}$ Shewhart-type schemes

The two-sided side-sensitive $SRR_{2-of-(h+1)}$ schemes gives a signal when *two* samples out of $h + 1$ consecutive samples fall in region A (or C), which are separated by at most $h - 1$ samples that fall in region B. The two-sided side-sensitive $SRR_{2-of-(h+1)}$ schemes have three regions, which are $A = [UCL, +\infty)$, $B = (LCL, UCL)$ and $C = (-\infty, LCL]$ (see Figure 1 (a)).

The probabilities of a charting statistic falling in regions A, B and C are given by:

$$\begin{aligned}
p_A(\delta) &= P(\bar{X} \geq UCL) = 1 - \frac{1}{[1 + (M + S(k + \delta\sqrt{n}))^c]^q} \\
p_B(\delta) &= P(LCL \leq \bar{X} \leq UCL) = \frac{1}{[1 + (M - S(k - \delta\sqrt{n}))^c]^q} - \frac{1}{[1 + (M + S(k + \delta\sqrt{n}))^c]^q} \\
p_C(\delta) &= P(\bar{X} \leq LCL) = \frac{1}{[1 + (M - S(k - \delta\sqrt{n}))^c]^q}
\end{aligned} \tag{10}$$

respectively.

The two-sided $IRR_{2-of-(h+1)}$ schemes signal when either a single sample mean falls in region 1 (or region 5) or when *two* out of $h + 1$ consecutive samples fall in region 2 (or region 4), which are separated by at most $h - 1$ samples that fall in region 3 (see Figure 1 (b)). The two-sided side-sensitive $IRR_{2-of-(h+1)}$ schemes have five regions, which are region 1 = $[UCL, +\infty)$, region 2 = $[UWL, UCL)$, region 3 = (LWL, UWL) , region 4 = $(LCL, UWL]$, and region 5 = $(-\infty, LCL]$ (see Figure 1 (b)).

The probabilities of a charting statistic falling in regions 1, 2, 3, 4 and 5 are given as follows

$$\begin{aligned}
p_1(\delta) &= P(\bar{X} \geq UCL) = 1 - \frac{1}{[1 + (M + S(k_2 + \delta\sqrt{n}))^c]^q} \\
p_2(\delta) &= P(UWL \leq \bar{X} \leq UCL) = \frac{1}{[1 + (M + S(k_1 + \delta\sqrt{n}))^c]^q} - \frac{1}{[1 + (M + S(k_2 + \delta\sqrt{n}))^c]^q} \\
p_3(\delta) &= P(LWL \leq \bar{X} \leq UWL) = \frac{1}{[1 + (M - S(k_1 - \delta\sqrt{n}))^c]^q} - \frac{1}{[1 + (M + S(k_1 + \delta\sqrt{n}))^c]^q} \\
p_4(\delta) &= P(LCL \leq \bar{X} \leq LWL) = \frac{1}{[1 + (M - S(k_2 - \delta\sqrt{n}))^c]^q} - \frac{1}{[1 + (M - S(k_1 - \delta\sqrt{n}))^c]^q} \\
p_5(\delta) &= P(\bar{X} \leq LCL) = \frac{1}{[1 + (M - S(k_2 - \delta\sqrt{n}))^c]^q}
\end{aligned} \tag{11}$$

respectively.

2.2 Transition probability matrices of the two-sided $SRR_{2-of-(h+1)}$ and $IRR_{2-of-(h+1)}$ side-sensitive schemes

Let us now consider the side-sensitive scheme of the two-sided $SRR_{2-of-(h+1)}$ schemes. When $h = 1$, it can be shown that the absorbing states are given by Λ , i.e. $\Lambda_1 = \{AA\}$ and $\Lambda_2 = \{CC\}$. When $h = 2$, the absorbing states are given by $\Lambda_1 = \{AA\}$, $\Lambda_2 = \{ABA\}$, $\Lambda_3 = \{CC\}$ and $\Lambda_4 = \{CBC\}$.

To evaluate the zero-state run-length properties of the $SRR_{2-of-(h+1)}$ side-sensitive schemes, the absorbing patterns Λ are decomposed into simple transient sub-patterns, denoted by η . In our example, when $h = 1$, $\eta_2 = \{A\}$ and $\eta_3 = \{B\}$. When $h = 2$, $\eta_1 = \{AB\}$, $\eta_2 = \{A\}$, $\eta_4 = \{C\}$ and $\eta_5 = \{CB\}$. Afterwards, create a dummy state, denoted by ϕ , defined by $\eta_3 = \{B\}$ for any value of h . Note that the dummy state is the $(h + 1)^{th}$ state in the essential TPM. For instance, when $h = 2$, $\varepsilon = 2 + 1 = 3$, which means that the dummy state is the 3rd state in the essential TPM (i.e. $\phi = \eta_\varepsilon = \eta_3 = \{B\}$). Finally, the state space, denoted by Ω , is the set of all the components. When $h = 1$, $\Omega = \{\eta_1; \phi; \eta_3; OOC\}$. For $h = 2$, $\Omega = \{\eta_1, \eta_2; \phi; \eta_4, \eta_5; OOC\}$. Table 1 presents the decomposition of the TPM's state space of the $SRR_{2-of-(h+1)}$ side-sensitive schemes when $h = 1, 2, 3$ and 4. The state space of the $IRR_{2-of-(h+1)}$ side-sensitive schemes of any h value is constructed in a similar way. For more details on the construction of the TPMs side-sensitive runs-rules, see Appendix.

Table 1. Decomposition of the TPM's state space of a two-sided $SRR_{2-of-(h+1)}$ side-sensitive schemes when $h = 1, 2, 3$ and 4

h	Λ	ϕ	η	Ω
1	$\Lambda_1=\{AA\}, \Lambda_2=\{CC\}$	$\eta_2=\{B\}$	$\eta_1=\{A\}, \eta_3=\{C\}$	$\{\eta_1; \phi; \eta_3; OOC\}$
2	$\Lambda_1=\{AA\}, \Lambda_2=\{ABA\}, \Lambda_3=\{CC\}, \Lambda_4=\{CBC\}$	$\eta_3=\{B\}$	$\eta_1=\{AB\}, \eta_2=\{A\}, \eta_4=\{C\}, \eta_5=\{CB\}$	$\{\eta_1, \eta_2; \phi; \eta_4, \eta_5; OOC\}$
3	$\Lambda_1=\{AA\}, \Lambda_2=\{ABA\}, \Lambda_3=\{ABBA\}, \Lambda_4=\{CC\}, \Lambda_5=\{CBC\}, \Lambda_6=\{CBBC\}$	$\eta_4=\{B\}$	$\eta_1=\{ABB\}, \eta_2=\{AB\}, \eta_3=\{A\}, \eta_5=\{C\}, \eta_6=\{CB\}, \eta_7=\{CBB\}$	$\{\eta_1, \eta_2, \eta_3; \phi; \eta_5, \eta_6, \eta_7; OOC\}$
4	$\Lambda_1=\{AA\}, \Lambda_2=\{ABA\}, \Lambda_3=\{ABBA\}, \Lambda_4=\{ABBBA\}, \Lambda_5=\{CC\}, \Lambda_6=\{CBC\}, \Lambda_7=\{CBBC\}, \Lambda_8=\{CBBBC\}$	$\eta_5=\{B\}$	$\eta_1=\{ABBB\}, \eta_2=\{ABB\}, \eta_3=\{AB\}, \eta_4=\{A\}, \eta_6=\{C\}, \eta_7=\{CB\}, \eta_8=\{CBB\}, \eta_9=\{CBBB\}$	$\{\eta_1, \eta_2, \eta_3, \eta_4; \phi; \eta_6, \eta_7, \eta_8, \eta_9; OOC\}$

Table 1 yields the TPMs in Table 2 using the look forward approach when $h = 1, 2$ and 3.

Table 2. The TPMs of the $SRR_{2-of-(h+1)}$ and $IRR_{2-of-(h+1)}$ side-sensitive schemes for $h = 1, 2, 3$ and 4

h	SRR _{2-of-(h+1)} schemes					IRR _{2-of-(h+1)} schemes												
1		η_1	ϕ	η_3	OOC		η_1	ϕ	η_3	OOC								
	η_1	0	p_B	p_C	p_A	η_1	0	p_1	p_2	$p_1 + p_2$								
	ϕ	p_A	p_B	p_C	0	ϕ	p_2	p_3	p_4	$p_1 + p_5$								
	η_3	p_A	p_B	0	p_C	η_3	p_2	p_3	0	$p_4 + p_1 + p_5$								
	OOC	0	0	0	1	OOC	0	0	0	1								
2		η_1	η_2	ϕ	η_4	η_5	OOC		η_1	η_2	ϕ	η_4	η_5	OOC				
	η_1	0	0	p_B	p_C	0	p_A	η_1	0	0	p_1	p_2	0	$p_1 + p_2$				
	η_2	p_B	0	0	p_C	0	p_A	η_2	p_3	0	0	p_4	0	$p_2 + p_1$				
	ϕ	0	p_A	p_B	p_C	0	0	ϕ	0	p_2	p_3	p_4	0	$p_1 + p_5$				
	η_4	0	p_A	0	0	p_B	p_C	η_4	0	p_2	0	0	p_3	$p_4 + p_1$				
	η_5	0	p_A	p_B	0	0	p_C	η_5	0	p_2	p_3	0	0	$p_4 + p_1$				
	OOC	0	0	0	0	0	1	OOC	0	0	0	0	0	1				
3		η_1	η_2	η_3	ϕ	η_5	η_6	η_7	OOC		η_1	η_2	η_3	ϕ	η_5	η_6	η_7	OOC
	η_1	0	0	0	p_B	p_C	0	0	p_A	η_1	0	0	0	p_1	p_2	0	0	$p_1 + p_2$
	η_2	p_B	0	0	0	p_C	0	0	p_A	η_2	p_3	0	0	0	p_4	0	0	$p_2 + p_1$
	η_3	0	p_B	0	0	p_C	0	0	p_A	η_3	0	p_3	0	0	p_4	0	0	$p_2 + p_1$
	ϕ	0	0	p_A	p_B	p_C	0	0	0	ϕ	0	0	p_2	p_3	p_4	0	0	$p_1 + p_5$
	η_5	0	0	p_A	0	0	p_B	0	p_C	η_5	0	0	p_2	0	0	p_3	0	$p_4 + p_1$
	η_6	0	0	p_A	0	0	0	p_B	p_C	η_6	0	0	p_2	0	0	p_3	p_4	$p_1 + p_2$
	η_7	0	0	p_A	p_B	0	0	0	p_C	η_7	0	0	p_2	p_3	0	0	0	$p_4 + p_1$
	OOC	0	0	0	0	0	0	0	1	OOC	0	0	0	0	0	0	0	1

Therefore, for any value of h the TPMs of the two-sided $SRR_{2-of-(h+1)}$ and $IRR_{2-of-(h+1)}$ side-sensitive schemes are given by

	η_1	η_2	\dots	η_{l-3}	η_{l-2}	η_{l-1}	ϕ	η_{l+1}	η_{l+2}	η_{l+3}	\dots	$\eta_{\tau-1}$	η_{τ}	OOC
η_1							p_B	p_C						p_A
η_2	p_B							p_C						p_A
η_3		p_B						p_C						p_A
\vdots			\ddots					\vdots						\vdots
η_{l-3}								p_C						p_A
η_{l-2}				p_B				p_C						p_A
η_{l-1}					p_B			p_C						p_A
ϕ						p_A	p_B	p_C						
η_{l+1}						p_A			p_B					p_C
η_{l+2}						p_A				p_B				p_C
η_{l+3}						p_A					\ddots			p_C
\vdots						\vdots								\vdots
$\eta_{\tau-2}$						p_A						p_B		p_C
$\eta_{\tau-1}$						p_A							p_B	p_C
η_{τ}						p_A	p_B							p_C
OOC														1

(12)

and

	η_1	η_2	\dots	η_{l-3}	η_{l-2}	η_{l-1}	ϕ	η_{l+1}	η_{l+2}	η_{l+3}	\dots	$\eta_{\tau-1}$	η_{τ}	OOC
η_1							p_3	p_4						$p_2 + p_1 + p_5$
η_2	p_3							p_4						$p_2 + p_1 + p_5$
η_3		p_3						p_4						$p_2 + p_1 + p_5$
\vdots			\ddots					\vdots						\vdots
η_{l-3}								p_4						$p_2 + p_1 + p_5$
η_{l-2}				p_3				p_4						$p_2 + p_1 + p_5$
η_{l-1}					p_3			p_4						$p_2 + p_1 + p_5$
ϕ						p_2	p_3	p_4						$p_1 + p_5$
η_{l+1}						p_2			p_3					$p_4 + p_1 + p_5$
η_{l+2}						p_2				p_3				$p_4 + p_1 + p_5$
η_{l+3}						p_2								$p_4 + p_1 + p_5$
\vdots						\vdots					\ddots			\vdots
$\eta_{\tau-3}$						p_2								$p_4 + p_1 + p_5$
$\eta_{\tau-2}$						p_2						p_3		$p_4 + p_1 + p_5$
$\eta_{\tau-1}$						p_2							p_3	$p_4 + p_1 + p_5$
η_{τ}						p_2	p_3							$p_4 + p_1 + p_5$
OOC														1

(13)

3. Run-length distribution of the two-sided $SRR_{2-of-(h+1)}$ and $IRR_{2-of-(h+1)}$ $BTXII$ Shewhart \bar{X} schemes

In this section, the expressions of the run-length distribution of the proposed schemes are derived using the Markov chain approach. Some extensions to the existing components of the proposed schemes are also presented.

The zero-state and steady-state run-length characteristics are mostly used to investigate the short-term and the long-term run-length properties of a monitoring scheme, respectively. The zero-state run-length is defined as the number of plotted points at which the chart first signals given that it begins in some specific initial state. However, the steady-state run-length is the number of points at which the chart first signals given that the process begins and stays IC for a long time then at some random time, an OOC is observed.

For any integer τ (with $\tau = 2h + 1$), using the Markov chain approach, Equations (12) and (13) can be written as follows

$$T_{(\tau+1) \times (\tau+1)} = \left(\begin{array}{c|c} Z_{\tau \times \tau} & \mathbf{r}_{\tau \times 1} \\ \hline \mathbf{0}'_{1 \times \tau} & \mathbf{1}_{1 \times 1} \end{array} \right) \quad (14)$$

where $Z = Z_{\tau \times \tau}$ is the essential TPM of the chart, $\mathbf{r} = \mathbf{1} - Z\mathbf{1}$ with $\mathbf{r} = \mathbf{r}_{\tau \times 1}$, $\mathbf{0}_{\tau \times 1} = (0 \ 0 \ \dots \ 0)'$ and $\mathbf{1} = \mathbf{1}_{\tau \times 1} = (1 \ 1 \ \dots \ 1)'$.

Therefore, the zero-state and steady-state run-length distributions of the proposed schemes are given by

$$\mathbf{P}(N = t) = \boldsymbol{\xi} \mathbf{Z}^{t-1} (\mathbf{I} - \mathbf{Z}) \mathbf{1} \text{ for } t = 1, 2, 3, \dots \text{ with } \mathbf{Z}^0 = \mathbf{I}, \quad (15)$$

where $\mathbf{I} = \mathbf{I}_{\tau \times \tau}$ and $\boldsymbol{\xi} = \boldsymbol{\xi}_{1 \times \tau}$. The zero-state and steady-state *ARL* of the proposed scheme are then given by

$$ARL(\delta) = \boldsymbol{\xi}_{1 \times \tau} \cdot \mathbf{ARL}_{\tau \times 1}(\delta), \quad (16)$$

where $\mathbf{ARL}_{\tau \times 1}(\delta) = (\mathbf{I}_{\tau \times \tau} - \mathbf{Z}_{\tau \times \tau}(\delta))^{-1} \cdot \mathbf{1}_{\tau \times 1}$.

The $\boldsymbol{\xi}_{1 \times \tau}$ vector of the side-sensitive $\text{SRR}_{2\text{-of-}(h+1)}$ scheme is given by

$$\boldsymbol{\xi}_{1 \times \tau} = \begin{cases} \mathbf{q}_{1 \times \tau} = (0 \ 0 \ \dots \ 0 \ 1 \ 0 \ \dots \ 0 \ 0) & \text{for zero-state mode} \\ \mathbf{s}_{1 \times \tau} & \text{for steady-state mode} \end{cases} \quad (17)$$

where the l^{th} ($l = \frac{\tau+1}{2}$) component of the zero-state vector is equal to one and zero elsewhere.

3.1 Characteristics of run-length distribution of the $\text{SRR}_{2\text{-of-}(h+1)}$ scheme

Using Equations (12), (16) and (17), the *ZSARL* of the two-sided $\text{SRR}_{2\text{-of-}(h+1)}$ side-sensitive scheme for any value of h is given by

$$ZSARL(\delta) = \frac{(1 + p_A \sum_{i=0}^{h-1} p_B^i)(1 + p_C \sum_{i=0}^{h-1} p_B^i)}{1 - p_B - p_A p_B^h - p_C p_B^h - p_A p_C \sum_{i=0}^{2h-1} p_B^i} \quad (18)$$

and the *SSARL* of the two-sided $\text{SRR}_{2\text{-of-}(h+1)}$ side-sensitive scheme for any value of h is given by

$$SSARL(\delta) = s_{h+1} \zeta_{h+1}(\delta) + \sum_{i=1}^h s_i \times (\zeta_i(\delta) + \zeta_{(2h+2)-i}(\delta)), \quad (19)$$

where

$$\mathbf{s}_{(1 \times \tau)} = \begin{pmatrix} s_1 \\ s_2 \\ s_3 \\ \vdots \\ s_{h-2} \\ s_{h-1} \\ s_h \\ s_{h+1} \\ s_{h+2} \\ s_{h+3} \\ s_{h+4} \\ \vdots \\ s_{2h-1} \\ s_{2h} \\ s_{2h+1} \end{pmatrix}' = \frac{1}{2 \sum_{i=0}^{h-1} \theta^i + 2\theta^h(1-p_B)^{-1}} \begin{pmatrix} \theta^{h-1} \\ \theta^{h-2} \\ \theta^{h-3} \\ \vdots \\ \theta^2 \\ \theta \\ 1 \\ 2\theta^h(1-p_2)^{-1} \\ 1 \\ \theta \\ \theta^2 \\ \vdots \\ \theta^{h-3} \\ \theta^{h-2} \\ \theta^{h-1} \end{pmatrix}' ,$$

respectively, with $\theta = \frac{2p_B}{1+p_B}$ and

$$\begin{aligned}
\mathbf{ARL}_{(\tau \times 1)}(\delta) &= \begin{pmatrix} \zeta_1(\delta) \\ \zeta_2(\delta) \\ \vdots \\ \zeta_{h-3}(\delta) \\ \zeta_{h-2}(\delta) \\ \zeta_{h-1}(\delta) \\ \zeta_h(\delta) \\ \zeta_{h+1}(\delta) \\ \zeta_{h+2}(\delta) \\ \zeta_{h+3}(\delta) \\ \zeta_{h+4}(\delta) \\ \zeta_{h+5}(\delta) \\ \vdots \\ \zeta_{2h}(\delta) \\ \zeta_{2h+1}(\delta) \end{pmatrix} = \frac{1}{\pi} \begin{pmatrix} \left(1 + p_A p_B \sum_{i=0}^{h-2} p_B^i\right) \left(1 + p_C \sum_{i=0}^{h-1} p_B^i\right) \\ \left(1 + p_A p_B^2 \sum_{i=0}^{h-3} p_B^i\right) \left(1 + p_C \sum_{i=0}^{h-1} p_B^i\right) \\ \vdots \\ \left(1 + p_A p_B^{h-3} \sum_{i=0}^2 p_B^i\right) \left(1 + p_C \sum_{i=0}^{h-1} p_B^i\right) \\ \left(1 + p_A p_B^{h-2} \sum_{i=0}^1 p_B^i\right) \left(1 + p_C \sum_{i=0}^{h-1} p_B^i\right) \\ \left(1 + p_A p_B^{h-1}\right) \left(1 + p_C \sum_{i=0}^{h-1} p_B^i\right) \\ 1 + p_C \sum_{i=0}^{h-1} p_B^i \\ \left(1 + p_A \sum_{i=0}^{h-1} p_B^i\right) \left(1 + p_C \sum_{i=0}^{h-1} p_B^i\right) \\ 1 + p_A \sum_{i=0}^{h-1} p_B^i \\ \left(1 + p_C p_B^{h-1}\right) \left(1 + p_A \sum_{i=0}^{h-1} p_B^i\right) \\ \left(1 + p_C p_B^{h-2} \sum_{i=0}^1 p_B^i\right) \left(1 + p_A \sum_{i=0}^{h-1} p_B^i\right) \\ \left(1 + p_C p_B^{h-3} \sum_{i=0}^2 p_B^i\right) \left(1 + p_A \sum_{i=0}^{h-1} p_B^i\right) \\ \vdots \\ \left(1 + p_C p_B^2 \sum_{i=0}^{h-3} p_B^i\right) \left(1 + p_A \sum_{i=0}^{h-1} p_B^i\right) \\ \left(1 + p_C p_B \sum_{i=0}^{h-2} p_B^i\right) \left(1 + p_A \sum_{i=0}^{h-1} p_B^i\right) \end{pmatrix}
\end{aligned}$$

with $\pi = 1 - p_B - p_A p_B^h - p_C p_B^h - p_A p_C \sum_{i=0}^{2h-1} p_B^i$.

3.2 Characteristics of the run-length distribution of the two-sided IRR_{2-of-(h+1)} side-sensitive scheme

Using Equations (13), (16) and (17), the *ZSARL* of the two-sided IRR_{2-of-(h+1)} side-sensitive scheme for any value of h is given by

$$ZSARL(\delta) = \frac{(1 + p_2 \sum_{i=0}^{h-1} p_3^i)(1 + p_4 \sum_{i=0}^{h-1} p_3^i)}{1 - p_3 - p_2 p_3^h - p_4 p_3^h - p_2 p_4 \sum_{i=0}^{2h-1} p_3^i}. \quad (20)$$

However, the expression of the steady-state ARL of the two-sided $IRR_{2-of-(h+1)}$ side-sensitive scheme for any value of h is given by

$$SSARL(\delta) = s_{h+1} \zeta_{h+1}(\delta) + \sum_{i=1}^h s_i \times (\zeta_i(\delta) + \zeta_{(2h+2)-i}(\delta)), \quad (21)$$

where

$$\begin{pmatrix} s_1 \\ s_2 \\ s_3 \\ \vdots \\ s_{h-2} \\ s_{h-1} \\ s_h \\ s_{h+1} \\ s_{h+2} \\ s_{h+3} \\ s_{h+4} \\ \vdots \\ s_{2h-1} \\ s_{2h} \\ s_{2h+1} \end{pmatrix} = \frac{1}{2 \sum_{i=0}^{h-1} \pi_1^i + 2\pi_1^h (1 - \pi_2)^{-1}} \begin{pmatrix} \pi_1^{h-1} \\ \pi_1^{h-2} \\ \pi_1^{h-3} \\ \vdots \\ \pi_1^2 \\ \pi_1 \\ 1 \\ 2\pi_1^h (1 - \pi_2)^{-1} \\ 1 \\ \pi_1 \\ \pi_1^2 \\ \vdots \\ \pi_1^{h-3} \\ \pi_1^{h-2} \\ \pi_1^{h-1} \end{pmatrix},$$

with $\pi_1 = \frac{p_3}{p_2 + p_3}$ and $\pi_2 = \frac{p_3}{p_3 + 2p_2}$, since for symmetric control limits, $p_2 = p_4$ when $\delta = 0$.

$$\begin{aligned}
\mathbf{ARL}_{(\tau \times 1)}(\delta) &= \begin{pmatrix} \zeta_1(\delta) \\ \zeta_2(\delta) \\ \vdots \\ \zeta_{h-3}(\delta) \\ \zeta_{h-2}(\delta) \\ \zeta_{h-1}(\delta) \\ \zeta_h(\delta) \\ \zeta_{h+1}(\delta) \\ \zeta_{h+2}(\delta) \\ \zeta_{h+3}(\delta) \\ \zeta_{h+4}(\delta) \\ \zeta_{h+5}(\delta) \\ \vdots \\ \zeta_{2h}(\delta) \\ \zeta_{2h+1}(\delta) \end{pmatrix} = \frac{1}{1 - p_3 - p_2 p_3^h - p_4 p_3^h - p_2 p_4 \sum_{i=0}^{2h-1} p_3^i} \begin{pmatrix} \left(1 + p_2 p_3 \sum_{i=0}^{h-2} p_3^i\right) \left(1 + p_4 \sum_{i=0}^{h-1} p_3^i\right) \\ \left(1 + p_2 p_3^2 \sum_{i=0}^{h-3} p_3^i\right) \left(1 + p_4 \sum_{i=0}^{h-1} p_3^i\right) \\ \vdots \\ \left(1 + p_2 p_3^{h-3} \sum_{i=0}^2 p_3^i\right) \left(1 + p_4 \sum_{i=0}^{h-1} p_3^i\right) \\ \left(1 + p_2 p_3^{h-2} \sum_{i=0}^1 p_3^i\right) \left(1 + p_4 \sum_{i=0}^{h-1} p_3^i\right) \\ \left(1 + p_2 p_3^{h-1}\right) \left(1 + p_4 \sum_{i=0}^{h-1} p_3^i\right) \\ 1 + p_4 \sum_{i=0}^{h-1} p_3^i \\ \left(1 + p_2 \sum_{i=0}^{h-1} p_3^i\right) \left(1 + p_4 \sum_{i=0}^{h-1} p_3^i\right) \\ 1 + p_2 \sum_{i=0}^{h-1} p_3^i \\ \left(1 + p_4 p_3^{h-1}\right) \left(1 + p_2 \sum_{i=0}^{h-1} p_3^i\right) \\ \left(1 + p_4 p_3^{h-2} \sum_{i=0}^1 p_3^i\right) \left(1 + p_2 \sum_{i=0}^{h-1} p_3^i\right) \\ \left(1 + p_4 p_3^{h-3} \sum_{i=0}^2 p_3^i\right) \left(1 + p_2 \sum_{i=0}^{h-1} p_3^i\right) \\ \vdots \\ \left(1 + p_4 p_3^2 \sum_{i=0}^{h-3} p_3^i\right) \left(1 + p_2 \sum_{i=0}^{h-1} p_3^i\right) \\ \left(1 + p_4 p_3 \sum_{i=0}^{h-2} p_3^i\right) \left(1 + p_2 \sum_{i=0}^{h-1} p_3^i\right) \end{pmatrix}.
\end{aligned}$$

3.3 The zero-state and steady-state average extra quadratic loss of the proposed schemes

The zero-state *AEQL* (*ZSAEQL*) and steady-state *AEQL* (*SSAEQL*) overall performances of the proposed side-sensitive schemes are defined by

$$ZSAEQL(\delta) = \frac{1}{\delta_{max} - \delta_{min}} \int_{\delta_{min}}^{\delta_{max}} \delta^2 \times ZSARL(\delta) \times f(\delta) d\delta \quad (22)$$

and

$$SSAEQL(\delta) = \frac{1}{\delta_{max} - \delta_{min}} \int_{\delta_{min}}^{\delta_{max}} \delta^2 \times SSARL(\delta) \times f(\delta) d\delta, \quad (23)$$

respectively, where $f(\delta)$ is the pdf of a uniform distribution with parameters 0 and 1.

4. Performance study

4.1 IC and OOC performance of the side-sensitive $SRR_{2-of-(h+1)}$ and $IRR_{2-of-(h+1)}$ BTXII Shewhart \bar{X} schemes

The computation of the control limits is one of the most important steps in the design of schemes. We considered the specified values of M , S , c and q proposed by Burr¹⁹ and Azam et al⁶ to design the proposed side-sensitive schemes. Therefore, the combination $(M, S, c, q) = (0.6295, 0.1856, 4.85437, 6.22665)$ is used to investigate the performance of the proposed control schemes. To compute the control limits, we need first to find the optimal schemes parameters k, k_1 and k_2 . The schemes parameters k, k_1 and k_2 of the side-sensitive $SRR_{2-of-(h+1)}$ and $IRR_{2-of-(h+1)}$ BTXII Shewhart \bar{X} schemes are computed using the following BTXII algorithm.

Step 1: Specify the size of the BTXII sample, n , the value of h, c, q, M, S , the number of replications, v , and the nominal IC $ZSARL$ ($ZSARL_0$) and IC $SSARL$ ($SSARL_0$). For instance, we can use $n = 5, 10$ and $25, h = 1, 2, \dots, 10, c = 4.85437, q = 6.22665, M = 0.6295, S = 0.1856, v = 100000$ and we set the nominal $ZSARL_0$ and $SSARL_0$ values at a high desired value such as 370 or 500.

Step 2: (a) For the $SRR_{2-of-(h+1)}$ side-sensitive schemes, set k to some value and compute the probabilities p_A, p_B and p_C using Equation (10) so that Equations (18) and (19) yield the desired nominal $ZSARL_0$ and $SSARL_0$. If the attained $ZSARL_0$ or $SSARL_0$ value is greater (lesser) than the expected (or desired) nominal value, then decrease (increase) the value of k until the attained $ZSARL_0$ or $SSARL_0$ is equal to the desired nominal (i.e. pre-specified) ARL_0 value.

(b) For the $IRR_{2-of-(h+1)}$ schemes, set k_1 to some value, compute the corresponding $k_2 (k_2 > k_1)$; and afterwards, compute the probabilities p_1, p_2, p_3, p_4 and p_5 using

Equation (11) so that Equations (20) and (21) yield the pre-specified $ZSARL_0$ and $SSARL_0$ values.

Step 3: From the values of the scheme parameters k, k_1 and k_2 found in Step 2, evaluate the IC and OOC performance in terms of the $ZSARL$ (or $SSARL$) values and compute the $ZSAEQL$ (or $SSAEQL$) values using either Equation (22) or (23) where $(\delta_{min}, \delta_{max}) = (0, 2.5)$ with an increment shift of 0.1 standard unit.

Step 4: Repeat Steps 2 and 3 v times (say 100000 times).

Step 5: Select the scheme parameters that yield a minimum $ZSAEQL$ (or $SSAEQL$) value. These parameters are called optimal scheme parameters.

Step 6: Use the optimal scheme parameters to compute the OOC $ZSARL$ ($ZSARL_\delta$) or OOC $SSARL$ ($SSARL_\delta$) by varying the mean shift ($\delta = 0.2 (0.2) 1.6$).

For instance, in Table 3 of zero-state mode, for a nominal $ZSARL_0$ value of 370.4 with $h = 1, 2$ and 3, it is found that $k = 1.5611, 1.6877$ and 1.7577 , respectively, so that the side-sensitive $SRR_{2-of-(h+1)}$ BTXII Shewhart \bar{X} scheme yields and an attained $ZSARL_0$ value of 370.4. However, for $h = 1, 2$ and 3, it is found that when $k_1 = 2.4, k_2 = 2.60531, 2.6058$ and 2.60629 , respectively, so that the side-sensitive $IRR_{2-of-(h+1)}$ BTXII Shewhart \bar{X} scheme yields and attained $ZSARL_0$ value of 370.4. For a nominal $ZSARL_0$ value of 500 with $h = 1, 2$ and 3, it is found that $k = 1.6213, 1.7457$ and 1.8148 , respectively, so that the side-sensitive $SRR_{2-of-(h+1)}$ BTXII Shewhart \bar{X} scheme yields and an attained $ZSARL_0$ value of 500. However, for $h = 1, 2$ and 3, it is found that when $k_1 = 2.4, k_2 = 2.6851, 2.6871$ and 2.6992 , respectively, so that the side-sensitive $IRR_{2-of-(h+1)}$ BTXII Shewhart \bar{X} scheme yields and attained $ZSARL_0$ value of 500. In steady-state mode, for a nominal $ZSARL_0$ value of 370.4 when $h = 1, 2$ and 3, it is found that $k = 1.56162, 1.68839$ and 1.75867 , respectively, so that the side-sensitive $SRR_{2-of-(h+1)}$ BTXII Shewhart \bar{X} scheme yields an attained $SSARL_0$ value of 370.4. However, for $h = 1, 2$ and 3, it is found that when $k_1 = 2.4, k_2 = 2.60532, 2.60581$ and 2.6063 , respectively, so that the side-sensitive $IRR_{2-of-(h+1)}$ BTXII Shewhart \bar{X} scheme yields an attained $SSARL_0$ value of 370.4. The zero-state and steady-state control limits and optimal parameters as well as the IC and OOC performances of the side-sensitive $SRR_{2-of-(h+1)}$ and $IRR_{2-of-(h+1)}$ BTXII Shewhart \bar{X} schemes are given in Tables 3 to 6.

Remark: The $ZSARL_0$ and $SSARL_0$ values of the proposed schemes as well as the basic scheme do not depend on the size of the sample (see for instance Equation (8) of the basic scheme).

From Tables 3 to 6, it can be seen that for both zero-state and steady-state modes, the distance between the CL and the control limits values is directly proportional to the value of h . For instance, in zero-state mode, for a nominal value of 370.4, the distance between the CL and the control limits of the $SRR_{2-of-(h+1)}$ control scheme for $h = 1, 3$ and 5 are equal to 0.2897, 0.3262 and 0.3418, respectively. It can also be observed that for a given nominal $ZSARL_0$ (or $SSARL_0$) value, when the distance between the CL and the warning limits (i.e., k_1) increases, the distance between the CL and the control limit (i.e., k_2) must be decreased in order to reach the required $ZSARL_0$ (or $SSARL_0$) value and vice versa.

Table 3. $ZSARL$ and $ZSAEQL$ values for the side-sensitive $SRR_{2-of-(h+1)}$ BTXII Shewhart \bar{X} schemes for $n = 5, 10$ and 25

n	Shift (δ)	Nominal $ARL_0 = 370.4$					Nominal $ARL_0 = 500$				
		1	2	h 3	4	5	1	2	h 3	4	5
5	0.0	370.40	370.40	370.40	370.40	370.40	500.00	500.00	500.00	500.00	500.00
	0.2	130.94	120.56	116.01	113.49	111.94	166.37	153.00	147.11	143.80	141.75
	0.4	29.91	26.61	25.42	24.89	24.65	35.67	31.53	30.00	29.27	28.91
	0.6	10.11	9.14	8.92	8.89	8.95	11.45	10.27	9.96	9.90	9.94
	0.8	4.84	4.52	4.51	4.58	4.66	5.25	4.87	4.84	4.90	4.98
	1.0	3.07	2.95	2.99	3.05	3.12	3.22	3.08	3.12	3.18	3.24
	1.6	2.04	2.04	2.05	2.06	2.07	2.05	2.04	2.05	2.06	2.06
	ZSAEQL	52.48	51.16	50.92	50.95	51.06	55.27	53.62	53.28	53.25	53.34
10	0.0	370.40	370.40	370.40	370.40	370.40	500.00	500.00	500.00	500.00	500.00
	0.2	67.86	61.03	58.23	56.76	55.92	83.83	75.12	71.48	69.53	68.37
	0.4	11.86	10.68	10.37	10.30	10.34	13.54	12.09	11.68	11.57	11.57
	0.6	4.23	3.99	4.00	4.07	4.15	4.55	4.26	4.25	4.32	4.40
	0.8	2.55	2.50	2.54	2.58	2.63	2.64	2.57	2.61	2.66	2.70
	1.0	2.12	2.11	2.13	2.14	2.16	2.14	2.13	2.15	2.17	2.18
	1.6	2.00	2.00	2.00	2.00	2.00	2.00	2.00	2.00	2.00	2.00
	ZSAEQL	43.89	43.42	43.34	43.35	43.38	44.87	44.29	44.17	44.15	44.18
25	0.0	370.40	370.40	370.40	370.40	370.40	500.00	500.00	500.00	500.00	500.00
	0.2	22.37	19.91	19.09	18.76	18.65	26.33	23.28	22.21	21.75	21.55
	0.4	3.78	3.59	3.61	3.68	3.76	4.03	3.80	3.82	3.88	3.96
	0.6	2.18	2.17	2.19	2.21	2.23	2.21	2.19	2.22	2.24	2.26
	0.8	2.01	2.01	2.01	2.02	2.02	2.00	2.01	2.02	2.02	2.02
	1.0	2.00	2.00	2.00	2.00	2.00	2.00	2.00	2.00	2.00	2.00
	1.6	2.00	2.00	2.00	2.00	2.00	2.00	2.00	2.00	2.00	2.00
	ZSAEQL	40.36	40.24	40.22	40.22	40.23	40.60	40.45	40.42	40.41	40.42
k	1.5611	1.6877	1.7577	1.8057	1.8419	1.6213	1.7457	1.8148	1.8622	1.8980	
LCL	0.3398	0.3163	0.3033	0.2944	0.2877	0.3286	0.3055	0.2927	0.2839	0.2772	
UCL	0.9192	0.9427	0.9557	0.9646	0.9713	0.9304	0.9535	0.9663	0.9751	0.9818	
CL(M, S, c, q)	0.6295 (0.6295, 0.1856, 4.85437, 6.22665)										

The findings in Table 3 show that in zero-state mode, regardless of the sample size, the addition of the standard side-sensitive $2-of-(h+1)$ runs-rules increases the sensitivity of the Shewhart-type BTXII \bar{X} scheme in the interval $0 < h \leq 3$ and reach the maximum efficiency when $h = 3$. The detection ability of the proposed side-sensitive $SRR_{2-of-(h+1)}$ schemes gradually

deteriorate as the value of h increases above 3 (i.e. $h > 3$) (see Table 3). Table 4 shows that in steady-state mode, when $n = 5$, the proposed $SRR_{2-of-(h+1)}$ side-sensitive scheme performs better for $h = 6$, which means that the addition of the side-sensitive runs-rules provides the maximum efficiency when $h = 6$, which is equivalent to SRR_{2-of-7} . For $n > 5$, it is more efficient to use large value of h . In other words, the more we add runs-rules (i.e. the more h is large), the better the efficiency of the scheme (see Table 4 and Figure 2). Tables 5 and 6 show that in both zero-state and steady-state modes, regardless of the sample size, the more h is large, the better the efficiency of the proposed side-sensitive $IRR_{2-of-(h+1)}$ BTXII Shewhart \bar{X} schemes. Moreover, Tables 3 to 6 show that for the $SRR_{2-of-(h+1)}$ side-sensitive schemes, the $ZSARL_\delta$ values converge toward two as the mean shift (δ) increases and the $SSARL_\delta$ values for large shifts are slightly less than two. Thus, for large shifts, it is recommended to use a minimum number of runs-rules on the standard $2-of-(h+1)$ schemes in order to keep the design and implementation as simple as possible. For the $IRR_{2-of-(h+1)}$ side-sensitive schemes, both the $ZSARL_\delta$ and $SSARL_\delta$ values converge toward one as δ increases. For large sample size, the larger the value of h , the better the performance of the proposed control charts for small shifts.

Table 4. $SSARL$ and $SSAEQL$ values for the side-sensitive $SRR_{2-of-(h+1)}$ BTXII Shewhart \bar{X} schemes for $n = 5, 10$ and 25

n	Shift (δ)	Nominal $ARL_0 = 370.4$					Nominal $ARL_0 = 500$				
		1	2	h 3	4	5	1	2	h 3	4	5
5	0.0	370.40	370.40	370.40	370.40	370.40	500.00	500.00	500.00	500.00	500.00
	0.2	130.76	120.29	115.67	113.08	111.45	166.19	152.74	146.77	143.39	141.26
	0.4	29.77	26.42	25.19	24.61	24.33	35.54	31.36	29.77	29.00	28.60
	0.6	10.02	9.03	8.77	8.72	8.75	11.37	10.16	9.83	9.74	9.75
	0.8	4.78	4.44	4.42	4.46	4.53	5.19	4.80	4.75	4.79	4.86
	1.0	3.02	2.89	2.92	2.96	3.01	3.17	3.03	3.05	3.10	3.15
	1.6	2.02	2.00	2.00	2.00	2.00	2.01	2.00	2.00	2.00	2.00
	SSAEQL	51.72	50.01	49.63	49.45	49.38	54.60	52.70	52.15	51.94	51.87
10	0.0	370.40	370.40	370.40	370.40	370.40	500.00	500.00	500.00	500.00	500.00
	0.2	67.69	60.79	57.92	56.39	55.48	83.65	74.88	71.17	69.16	67.94
	0.4	11.77	10.55	10.21	10.12	10.13	13.46	11.98	11.54	11.39	11.37
	0.6	4.18	3.91	3.91	3.96	4.02	4.50	4.19	4.17	4.22	4.29
	0.8	2.51	2.44	2.47	2.50	2.53	2.60	2.52	2.55	2.58	2.62
	1.0	2.08	2.06	2.07	2.07	2.08	2.11	2.09	2.09	2.10	2.11
	1.6	1.94	1.92	1.91	1.90	1.89	1.97	1.96	1.95	1.94	1.93
	SSAEQL	43.17	42.41	42.11	41.93	41.81	44.25	43.42	43.10	42.93	42.81
25	0.0	370.40	370.40	370.40	370.40	370.40	500.00	500.00	500.00	500.00	500.00
	0.2	22.24	19.75	18.89	18.52	18.36	26.21	23.12	22.01	21.51	21.28
	0.4	3.73	3.52	3.53	3.58	3.64	3.99	3.74	3.74	3.79	3.86
	0.6	2.14	2.12	2.13	2.14	2.15	2.18	2.15	2.16	2.18	2.19
	0.8	1.97	1.96	1.95	1.94	1.94	1.98	1.97	1.96	1.96	1.95
	1.0	1.96	1.95	1.94	1.93	1.92	1.97	1.96	1.94	1.94	1.93
	1.6	1.93	1.92	1.91	1.90	1.89	1.97	1.96	1.94	1.94	1.93
	AEQL	39.65	39.25	39.02	38.84	38.69	39.99	39.59	39.38	39.22	39.09
k	1.5616	1.6884	1.7587	1.8068	1.8432	1.6217	1.7462	1.8155	1.8630	1.8990	
LCL	0.3397	0.3161	0.3031	0.2942	0.2874	0.3285	0.3054	0.2925	0.2837	0.2770	
UCL	0.9193	0.9429	0.9559	0.9649	0.9716	0.9305	0.9536	0.9665	0.9753	0.9820	
CL(M, S, c, q)	0.6295 (0.6295, 0.1856, 4.85437, 6.22665)										

Table 5. ZSARL and ZSAEQL values for the side-sensitive IRR_{2-of-(h+1)} BTXII Shewhart \bar{X} schemes for $n = 5, 10$ and 25 with $k_1 = 2.4$

n	Shift (δ)	Nominal $ARL_0 = 370.4$					Nominal $ARL_0 = 500$				
		1	2	h 3	4	5	1	2	h 3	4	5
5	0.0	370.40	370.40	370.40	370.40	370.40	500.00	500.00	500.00	500.00	500.00
	0.2	186.03	185.41	184.80	184.20	183.63	254.16	252.36	250.63	248.96	247.35
	0.4	45.70	45.28	44.90	44.55	44.23	57.04	56.00	55.07	54.24	53.48
	0.6	14.91	14.70	14.54	14.40	14.28	17.52	17.05	16.69	16.39	16.15
	0.8	6.24	6.14	6.08	6.03	6.00	7.01	6.82	6.69	6.60	6.54
	1.0	3.20	3.16	3.14	3.13	3.13	3.48	3.41	3.37	3.35	3.34
	1.6	1.15	1.15	1.15	1.15	1.15	1.20	1.20	1.20	1.20	1.20
	ZSAEQL	42.12	41.9	41.73	41.59	41.48	47.49	46.98	46.61	46.30	46.05
10	0.0	370.40	370.40	370.40	370.40	370.40	500.00	500.00	500.00	500.00	500.00
	0.2	101.30	100.71	100.16	99.62	99.12	132.80	131.23	129.74	128.35	127.04
	0.4	17.72	17.49	17.29	17.13	16.98	21.00	20.47	20.04	19.68	19.38
	0.6	5.21	5.14	5.09	5.05	5.03	5.81	5.65	5.56	5.49	5.45
	0.8	2.28	2.26	2.25	2.25	2.25	2.44	2.40	2.39	2.39	2.38
	1.0	1.39	1.39	1.39	1.39	1.39	1.45	1.45	1.45	1.45	1.45
	1.6	1.00	1.00	1.00	1.01	1.00	1.00	1.00	1.00	1.00	1.00
	ZSAEQL	27.57	27.49	27.43	27.38	27.34	29.48	29.30	29.16	29.06	28.97
25	0.0	370.40	370.40	370.40	370.40	370.40	500.00	500.00	500.00	500.00	500.00
	0.2	34.18	33.82	33.51	33.22	32.96	41.97	41.11	40.35	39.69	39.10
	0.4	4.44	4.38	4.34	4.32	4.30	4.91	4.79	4.72	4.67	4.64
	0.6	1.54	1.53	1.53	1.53	1.53	1.61	1.60	1.60	1.60	1.60
	0.8	1.07	1.07	1.07	1.07	1.07	1.08	1.08	1.08	1.08	1.08
	1.0	1.00	1.00	1.00	1.00	1.00	1.01	1.01	1.01	1.01	1.01
	1.6	1.00	1.00	1.00	1.00	1.00	1.00	1.00	1.00	1.00	1.00
	ZSAEQL	21.6	21.58	21.56	21.55	21.54	22.07	22.02	21.99	21.96	21.94
k_2	2.6053	2.6058	2.6063	2.6068	2.6073	2.6851	2.6861	2.6871	2.6882	2.6992	
LCL ₂	0.1460	0.1459	0.1458	0.1457	0.1456	0.1311	0.1310	0.1308	0.1306	0.1304	
UCL ₂	1.1130	1.1131	1.1132	1.1133	1.1134	1.1279	1.1280	1.1282	1.1284	1.1286	
(LCL ₁ , UCL ₁)	(0.1841, 1.0749)										
CL(M, S, c, q)	0.6295 (0.6295, 0.1856, 4.85437, 6.22665)										

Table 6. SSARL and SSAEQL values for the side-sensitive IRR_{2-of-(h+1)} BTXII Shewhart \bar{X} schemes for $n = 5, 10$ and 25 with $k_1 = 2.4$

n	Shift (δ)	Nominal $ARL_0 = 370.4$					Nominal $ARL_0 = 500$				
		1	2	h 3	4	5	1	2	h 3	4	5
5	0.0	370.40	370.40	370.40	370.40	370.40	500.00	500.00	500.00	500.00	500.00
	0.2	186.03	185.40	184.79	184.19	183.61	254.15	252.35	250.61	248.94	247.32
	0.4	45.70	45.28	44.89	44.54	44.21	57.04	56.00	55.06	54.22	53.45
	0.6	14.91	14.70	14.53	14.39	14.27	17.51	17.05	16.68	16.38	16.13
	0.8	6.23	6.14	6.08	6.03	5.99	7.01	6.82	6.69	6.59	6.53
	1.0	3.20	3.16	3.14	3.13	3.12	3.48	3.41	3.37	3.35	3.33
	1.6	1.15	1.15	1.15	1.15	1.15	1.20	1.20	1.20	1.20	1.20
	SSAEQL	42.11	41.89	41.72	41.58	41.46	47.49	46.97	46.59	46.28	46.02
10	0.0	370.40	370.40	370.40	370.40	370.40	500.00	500.00	500.00	500.00	500.00
	0.2	101.30	100.71	100.15	99.61	99.10	132.80	131.22	129.73	128.33	127.00
	0.4	17.72	17.49	17.29	17.12	16.97	21.00	20.47	20.03	19.67	19.36
	0.6	5.21	5.13	5.08	5.05	5.02	5.81	5.65	5.55	5.49	5.44
	0.8	2.28	2.26	2.25	2.25	2.25	2.44	2.40	2.39	2.38	2.38
	1.0	1.39	1.39	1.39	1.39	1.39	1.45	1.45	1.45	1.45	1.45
	1.6	1.00	1.00	1.00	1.00	1.00	1.00	1.00	1.00	1.00	1.00
	SSAEQL	27.57	27.49	27.43	27.39	27.34	29.47	29.29	29.16	29.05	28.95
25	0.0	370.40	370.40	370.40	370.40	370.40	500.00	500.00	500.00	500.00	500.00
	0.2	34.18	33.82	33.50	33.21	32.94	41.96	41.10	40.34	39.67	39.07
	0.4	4.44	4.38	4.34	4.32	4.30	4.91	4.79	4.71	4.66	4.63
	0.6	1.54	1.53	1.53	1.53	1.53	1.61	1.60	1.60	1.60	1.60
	0.8	1.07	1.07	1.07	1.07	1.07	1.08	1.08	1.08	1.08	1.08
	1.0	1.00	1.00	1.00	1.00	1.00	1.01	1.01	1.01	1.01	1.01
	1.6	1.00	1.00	1.00	1.00	1.00	1.00	1.00	1.00	1.00	1.00
	SSAEQL	21.6	21.58	21.56	21.55	21.54	22.07	22.02	21.99	21.96	21.94
k_2	2.60532	2.60581	2.60630	2.60680	2.60729	2.6851	2.6861	2.6872	2.6882	2.6892	

LCL_2	0.1460	0.1459	0.1458	0.1457	0.1456	0.1311	0.1310	0.1308	0.1306	0.1304
UCL_2	1.1130	1.1131	1.1132	1.1133	1.1134	1.1279	1.1280	1.1282	1.1284	1.1286
(LCL_1, UCL_1)	(0.1841, 1.0749)									
$CL(M, S, c, q)$	0.6295 (0.6295, 0.1856, 4.85437, 6.22665)									

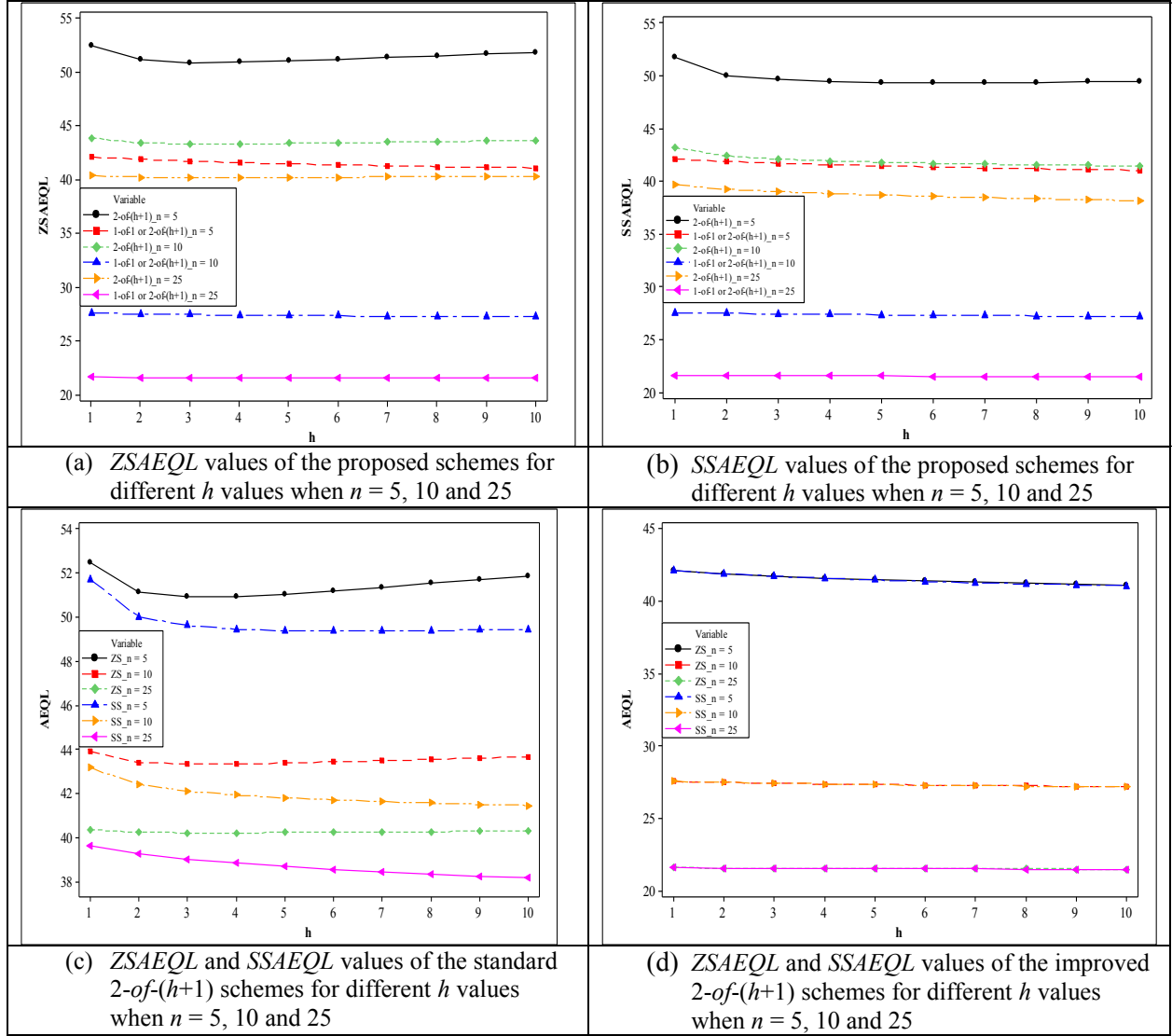


Figure 2. Zero-state and steady-state overall performances of the $SRR_{2-of-(h+1)}$ and $IRR_{2-of-(h+1)}$ side-sensitive schemes

Figure 2 presents the zero-state and the steady-state overall performance of the proposed side-sensitive schemes for $(\delta_{min}, \delta_{max}) = (0, 2.5)$. From Figures 2 (a)-(b), it can be seen that in both zero-state and steady-state modes, the improved scheme performs better than the standard scheme regardless of the value of h . The larger the sample size, the better the performance. Figure 2 (c) shows that the proposed standard side-sensitive schemes are more sensitive in steady-state mode and relatively less sensitive in zero-state mode. The improved side-sensitive schemes perform similarly in zero-state and steady-state modes when the sample size is the

same (see Figure 2 (d)). It can also be observed that the addition of runs-rules does not necessary improve the performance of the schemes. Therefore, a thorough investigation of the performance of the schemes is needed in order to find a specific scheme that provides a maximum efficiency. For instance, if $n = 5$, it is found that the side-sensitive $SRR_{2-of-(h+1)}$ BTXII Shewhart \bar{X} scheme performs better when $h = 3$.

4.2 Performance comparison

In Figure 3, the side-sensitive schemes (including other modifications of the side-sensitive schemes) are compared with the well-known traditional and synthetic Shewhart \bar{X} , \bar{X} -CUSUM and \bar{X} -EWMA schemes as well as the BTXII \bar{X} -CUSUM and \bar{X} -EWMA schemes. The comparison is done under symmetric and heavy-tailed distributions. Under symmetric distributions, and more precisely under the standard normal distribution, when the smoothing parameter λ of the classical \bar{X} -EWMA control chart is equal to 0.1 and 0.5, it is found that the optimal parameter $L = 2.698$ and 2.977 so that the attained $ZSARL_0 = 369.90$ and 368.90 , respectively, for a nominal $ZSARL_0$ value of 370.4 (see Figure 3 (a)). Under heavy-tailed distributions, and more specifically under the $GAM(1,1)$ distribution, the optimal parameters 2.698 and 2.977 yield $ZSARL_0$ values of 271.40 and 77.20 when $\lambda = 0.1$ and 0.5 , respectively. These results show that the \bar{X} -EWMA chart is not IC robust because the attained $ZSARL_0$ values of 271.40 and 77.20 are far different from the nominal $ZSARL_0$ value of 370.4 . For the classical \bar{X} -CUSUM control chart, we found that the UCL value is equal to 13.26 so that the attained $ZSARL_0$ value under the $N(0,1)$ distribution is equal to 369.5 . However, under the $GAM(1,1)$ distribution, when $UCL = 13.26$, the \bar{X} -CUSUM control chart yields an attained $ZSARL_0$ value of 301.27 , which shows that the classical \bar{X} -CUSUM chart is not IC robust as well.

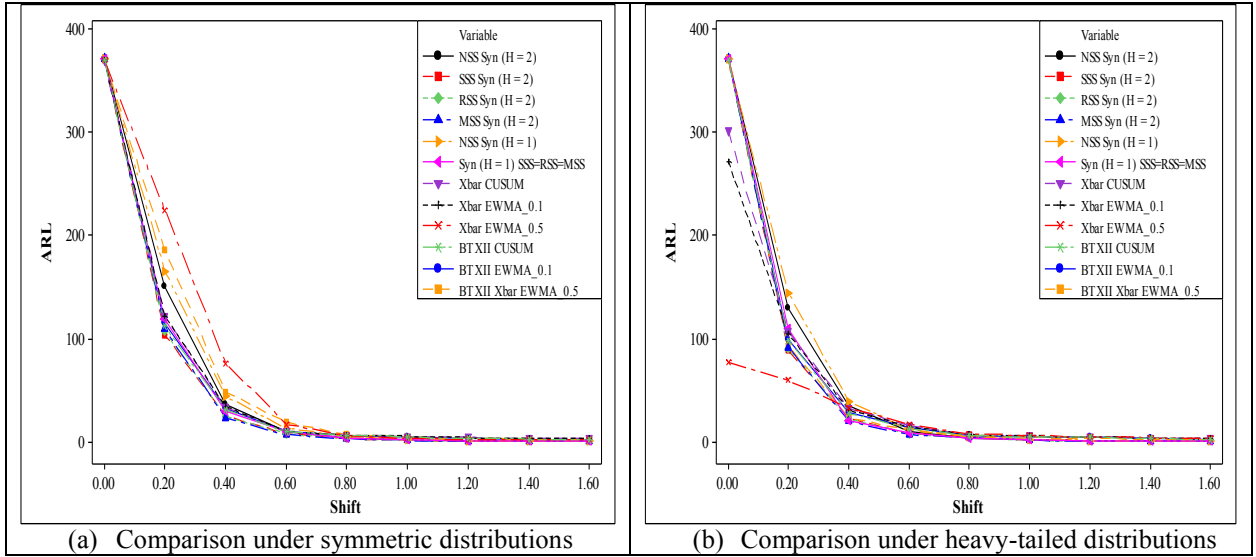


Figure 3. The *ARL* comparison of twelve schemes under symmetric and heavy-tailed distributions

From Figure 3 we can draw the following conclusions:

- Under symmetric distributions, when $h = 1$ and 2 , the classical and BTXII \bar{X} -EWMA control chart outperforms the NSS synthetic control chart for small values of λ under small and moderate shifts. When λ increases, the NSS synthetic scheme outperforms both the classical and BTXII \bar{X} -EWMA schemes regardless of the size of the mean shifts (see Figure 3 (a) when $\lambda = 0.1$).
- Under heavy-tailed distributions, when $h = 1$ and 2 , both classical and BTXII \bar{X} -EWMA and \bar{X} -CUSUM schemes outperform the NSS $SRR_{2-of-(h+1)} \bar{X}$ schemes regardless of the values of λ for small and moderate shifts (see Figure 3 (b)). For large shifts, the side-sensitive BTXII synthetic \bar{X} scheme performs better than classical and BTXII \bar{X} -EWMA and \bar{X} -CUSUM schemes.
- Under symmetric distributions and for large mean shifts, when $h = 1$, the traditional and BTXII side-sensitive $IRR_{2-of-(h+1)}$ as well as the basic Shewhart \bar{X} schemes are equivalent and perform better than the classical and BTXII \bar{X} -EWMA and \bar{X} -CUSUM schemes regardless of the size of the shifts.
- Under heavy-tailed distributions, the proposed side-sensitive $IRR_{2-of-(h+1)}$ BTXII \bar{X} and synthetic BTXII \bar{X} schemes outperform the classical \bar{X} -EWMA and \bar{X} -CUSUM schemes for two reasons, (i) they are IC robustness and (ii) yield small OOC *ARL* values. It can also be observed that the proposed side-sensitive \bar{X} schemes are more sensitive than the BTXII \bar{X} -EWMA and \bar{X} -CUSUM schemes.

- Under symmetric and heavy-tailed distributions, when $h = 2$, the proposed side-sensitive $IRR_{2-of-(h+1)} \bar{X}$ and $2-of-(h+1)$ synthetic BTXII schemes perform better than the classical \bar{X} -EWMA and \bar{X} -CUSUM schemes.
- The BTXII \bar{X} -EWMA and \bar{X} -CUSUM schemes perform uniformly better than the classical \bar{X} -EWMA and \bar{X} -CUSUM schemes under symmetric and heavy-tailed distributions regardless of the size of the location parameter.

5. Illustrative example

In this section, the design and implementation of the proposed schemes are illustrated using the dataset from Abbas et al.²² The data represent the shaft diameter which is expected to be around 7.995 millimetres (*mm*). To assess the production process, measurements of twenty-five samples have been taken, each consist of five items from the final production stage for which a goodness of fit test for normality is rejected.

For a nominal $ZSARL_0$ of 370.4, the ZS LCL and UCL of the proposed side-sensitive $SRR_{2-of-(h+1)}$ BTXII \bar{X} schemes when $h = 1$ and 2 (i.e., SRR_{2-of-2} and SRR_{2-of-3} schemes) are given by $(LCL, UCL) = (0.453, 0.731)$ and $(0.439, 0.745)$, respectively. A plot of the charting statistics is shown in Figure 4 (a). The ZS LCL and UCL of the traditional side-sensitive $SRR_{2-of-(h+1)} \bar{X}$ schemes when $h = 1$ and 2 are given by $(LCL, UCL) = (7.985, 7.994)$. A plot of the \bar{X} charting statistics is shown in Figure 4 (b). It can be seen that for both BTXII and traditional \bar{X} schemes, the SRR_{2-of-2} and SRR_{2-of-3} schemes do not signal in the prospective phase.

The ZS control and warning limits (LCL, UCL) and (LWL, UWL) of the proposed side-sensitive $IRR_{2-of-(h+1)}$ BTXII \bar{X} schemes are given by $(0.383, 0.804)$ and $(0.400, 0.787)$, respectively, when $h = 1$. However, the zero-state control and warning limits (LCL, UCL) and (LWL, UWL) of the side-sensitive $IRR_{2-of-(h+1)}$ traditional \bar{X} schemes are given by $(7.984, 8.000)$ and $(7.985, 7.999)$, respectively, when $h = 1$. A plot of the BTXII and traditional \bar{X} charting statistics are shown in Figures 4 (a) and (b), respectively. It can be seen that the proposed SRR_{2-of-2} BTXII scheme signal for the first time on the fourth sample; whereas, the traditional side-sensitive SRR_{2-of-2} schemes does not signal in the prospective phase.

The illustrative example demonstrates the superiority of the proposed schemes over the traditional schemes.

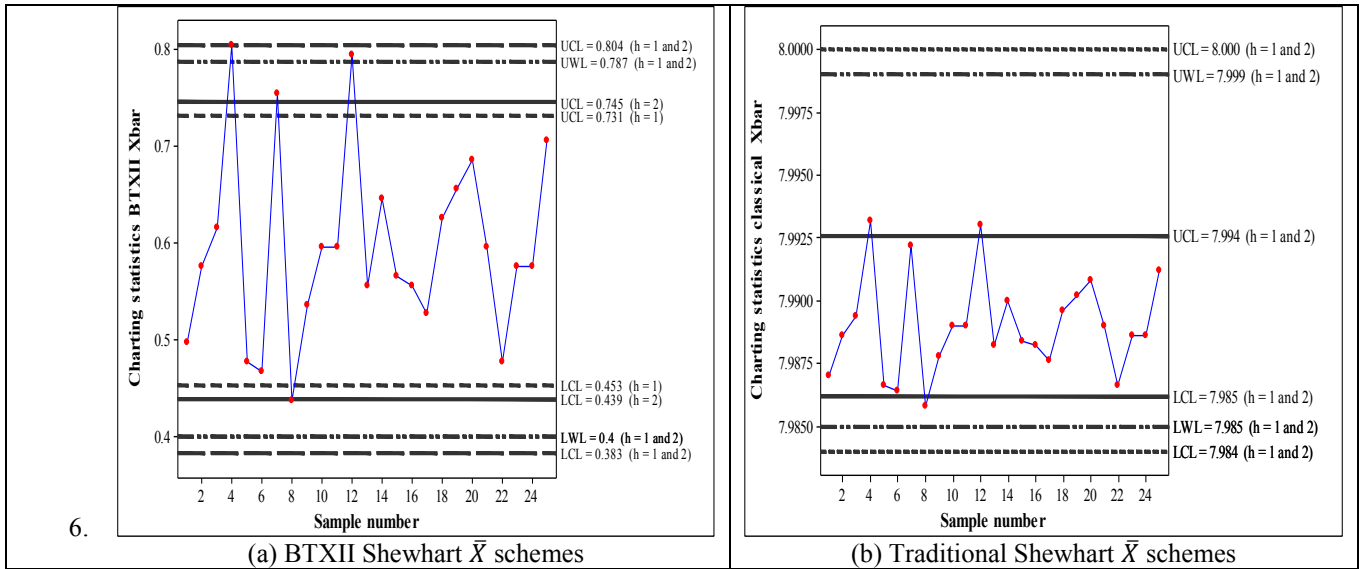


Figure 4. Side-sensitive $SRR_{2-of-(h+1)}$ and $IRR_{2-of-(h+1)}$ BTXII Shewhart \bar{X} and traditional Shewhart \bar{X} schemes of the measurements of shaft diameter in zero-state mode

7. Conclusion and summary

Shongwe and Graham¹⁵ investigated NSS and various side-sensitive runs-rules and synthetic \bar{X} schemes for normally distributed data. Malela-Majika et al³ proposed NSS $SRR_{2-of-(h+1)}$ and $IRR_{2-of-(h+1)}$ \bar{X} schemes for non-normal data. In this paper, we proposed side-sensitive $SRR_{2-of-(h+1)}$ and $IRR_{2-of-(h+1)}$ Shewhart-type \bar{X} schemes for non-normal data as alternative to the traditional side-sensitive $SRR_{2-of-(h+1)}$ and $IRR_{2-of-(h+1)}$ Shewhart-type \bar{X} schemes when the assumption of normality fail to hold. The zero-state and steady-state performance of the proposed schemes are investigated using the Markov chain approach. It was observed that the proposed schemes outperform the traditional ones, and present very interesting run-length characteristics under the normal and non-normal distributions. Moreover, the proposed side-sensitive schemes outperform the NSS schemes proposed by Malela-Majika et al.³ Practitioners in the industries are recommended to use the proposed schemes instead of the traditional schemes when the process is not stable or when there are doubts about the nature of the underlying distribution. When small and moderate shifts are of interest, it is recommended to use the side-sensitive $SRR_{2-of-(h+1)}$ schemes regardless of the size of the sample. For large shifts, it is recommended to use the side-sensitive $IRR_{2-of-(h+1)}$ schemes.

In future we will consider the design non-side-sensitive and side-sensitive Synthetic Shewhart-type \bar{X} schemes for non-normal data under the assumptions of known and unknown process parameters.

Acknowledgements

The authors thank Mr Shongwe Sandile for his valuable comments that helped to improve this article.

References

1. Montgomery DC. *Introduction to Statistical Quality Control*. 7th ed. John Wiley, New York, NY 2009.
2. Chakraborti, S., Eryilmaz, S., and S.W. Human. A phase II nonparametric control chart based on precedence statistics with runs-type signaling rules. *Computational Statistics and Data Analysis* 2009; **53**(4): 1054-1065.
3. Malela-Majika JC, Kanyama BJ, Rapoo EM. Improved Shewhart-type \bar{X} control schemes under non-normality assumption: A Markov chain approach. *International Journal of Quality Research* 2017; **12**(1): 17-42.
4. Guo B, Wang BX. Control charts for monitoring the Weibull shape parameter based on type II-censored sample. *Quality and Reliability Engineering International* 2014; **30**(1): 13-24.
5. Chen, JT. A Shewhart-type control scheme to monitor Weibull data without subgrouping. *Quality and Reliability Engineering International* 2014; **30**(8): 1197-1214.
6. Azam M, Ahmad L, Aslam M. Design of \bar{X} chart for Burr Distribution under the repetitive sampling. *Science International (Lahore)* 2016; **28**(4): 3265-3271.
7. Bizuneh B, Wang FK. Comparison of different control charts for a Weibull process with type-I censoring. *Communications in Statistics- Simulation and Computation* 2017; DOI: 10.1080/03610918.2017.1406508.
8. Champ CW, Woodall WH. Exact results for Shewhart control charts with supplementary run rules. *Technometrics* 1987; **29**(4): 393-399.
9. Reynolds Jr MR, Amin RW, Arnold JC, Nachlas JA. \bar{X} charts with variable sampling intervals. *Technometrics* 1988; **30**: 181-192.
10. Khoo MBC. Design of runs rules schemes. *Quality Engineering* 2003; **16**(1): 27-43.
11. Khoo MBC, Ariffin KN. Two improved runs-rules for Shewhart \bar{X} control chart. *Quality Engineering* 2006; **18**(2): 173-178.

12. Acosta-Mejia, CA. Two sets of runs rules for \bar{X} chart. *Quality Engineering* 2007; **19**: 129-136.
13. Koutras MV, Bersimis S, Maravelakis, PE. Statistical Process Control using Shewhart control chart with supplementary runs. *Methodology and Computing in Applied probability* 2007; **9**(2): 207-224.
14. Davis, RB and Woodall, WH. 1988. Performance of the Control Chart Trend Rule under Linear Shift. *Journal of Quality Technology* 1988; **20**(4): 260-262.
15. Shongwe SC, Graham, MA. On the performance of Shewhart-type synthetic and runs-rules charts combined with an \bar{X} chart. *Quality and Reliability Engineering International* 2016; **32**(4): 1357-1379.
16. Shongwe, SC, Graham, MA. Synthetic and runs-rules charts combined with an \bar{X} chart: theoretical discussion. *Quality and Reliability Engineering International* 2017; **33**(1): 7-35.
17. Mehmood R, Qazi MS, Riaz, M. On the performance of \bar{X} control chart for known and unknown parameters supplemented with runs rules under different probability distributions. *Journal of Statistical Computation and Simulations* 2018; **88**(4): 675-711.
18. Tran KP. Designing of run rules t charts for monitoring changes in the process mean. *Chemometrics and Intelligent Laboratory System* 2018; **174**: 85-93.
19. Burr IW. Cumulative frequency functions. *Annals of Mathematical Statistics* 1942; **13**(2): 215-232.
20. Chen Y-K. An evolutionary economic-statistical design for VSI \bar{X} control charts under non-normality. *International Journal of Advanced Manufacturing Technology* 2003; **22**: 602-610.
21. Burr IW. Parameters for general system of distributions to match a grid of α_3 and α_4 . *Communication in Statistics* 1973; **2**: 1-21.
22. Abbas MM, Ali, SA. Process capability evaluation for a non-normal distributed one. *Engineering and Technology Journal* 2013; **31**(17): 2345-2358.

APPENDIX

TPMs of the side-sensitive $SRR_{2-of-(h+1)}$ and $IRR_{2-of-(h+1)}$ schemes

This appendix explains how the Markov chain approach is used for the side-sensitive $SRR_{2-of-(h+1)}$ schemes. Let Y_i (where $i \geq 1$) be a sequence of iid random variables taking values in the set $V = \{1, 2, 3\}$ and let $P(Y_i = v) = p_v$ (for $1 \leq v \leq 3$). Let $v = 2$ denote a conforming state (i.e., the charting statistic falls between the LCL and UCL) of the proposed scheme; while, $v = 1$ and 3 denote the upper and lower non-conforming states, respectively (see Figure 1 (a) where $A \equiv 1$, $B \equiv 2$ and $C \equiv 3$). In this appendix, digits 1, 2 and 3 are used to symbolise different states, which are related to regions A, B and C, respectively. For example, 1233 indicates that in a sequence of four test samples, the first is an upper non-conforming (i.e., the charting statistic of this sample plots on or above the UCL in region A), the second is a conforming sample (i.e. the charting statistic plot in region B), and the third and fourth samples are lower non-conforming samples (i.e., their charting statistics plot on or below the LCL in region C). The digit on the right end of the series denotes the state of the most recent test sample while digits to the left represent the states observed in earlier samples.

Let us consider the case where $h = 1, 2, 3$ and 4 . The compound pattern gives all possible ways of obtaining an OOC signal using the $2-of-(h+1)$ schemes. Let Λ represents the set of compound (or absorbing) patterns. Let us consider the compound patterns of the side-sensitive $SRR_{2-of-(h+1)}$ schemes for $h = 1, 2, 3$ and 4 . In this case, the Markov chain states are obtained as follows:

Step 1: List all the absorbing patterns, Λ , given by

$$\Lambda = \{\Lambda_1 = \{AA\}, \Lambda_2 = \{CC\}\} \text{ for } h = 1$$

$$\Lambda = \{\Lambda_1 = \{AA\}, \Lambda_2 = \{ABA\}, \Lambda_3 = \{CC\}, \Lambda_4 = \{CBC\}\} \text{ for } h = 2$$

(A.1)

$$\Lambda = \{\Lambda_1 = \{AA\}, \Lambda_2 = \{ABA\}, \Lambda_3 = \{ABBA\}, \Lambda_4 = \{CC\}, \Lambda_5 = \{CBC\}, \Lambda_6 = \{CBBC}\} \text{ for } h = 3$$

$$\Lambda = \{\Lambda_1 = \{AA\}, \Lambda_2 = \{ABA\}, \Lambda_3 = \{ABBA\}, \Lambda_4 = \{ABBBA\}, \Lambda_5 = \{CC\}, \Lambda_6 = \{CBC\}, \Lambda_7 = \{CBBC\}, \Lambda_8 = \{CBBBC}\} \text{ for } h = 4$$

Step 2: Create the dummy state denoted by ϕ which is defined by the single IC state given by $\{2\}$ for any value of h . Thus, the dummy state are defined by

$$\begin{aligned}
\phi &= \eta_2 = \{B\} \text{ for } h = 1 \\
\phi &= \eta_3 = \{B\} \text{ for } h = 2 \\
\phi &= \eta_4 = \{B\} \text{ for } h = 3 \\
\phi &= \eta_5 = \{B\} \text{ for } h = 4
\end{aligned} \tag{A.2}$$

Therefore, $\phi = \eta_{h+1} = \{B\}$ for any value of h .

Step 3: Decompose each element in the absorbing patterns given in Equation (A.1) into its basic (i.e., transient sub-patterns) states by removing the last state.

$$\{\eta_1 = \{A\}, \eta_3 = \{C\}\} \text{ for } h = 1$$

$$\{\eta_1 = \{AB\}, \eta_2 = \{A\}, \eta_4 = \{C\}, \eta_5 = \{CB\}\} \text{ for } h = 2$$

(A.3)

$$\{\eta_1 = \{ABB\}, \eta_2 = \{AB\}, \eta_3 = \{A\}, \eta_5 = \{C\}, \eta_6 = \{CB\}, \eta_7 = \{CBB\}\} \text{ for } h = 3$$

$$\begin{aligned}
\{\eta_1 = \{ABBB\}, \eta_2 = \{ABB\}, \eta_3 = \{AB\}, \eta_4 = \{A\}, \eta_6 = \{C\}, \eta_7 = \{CB\}, \eta_8 = \\
\{CBB\}, \eta_9 = \{CBBB}\} \text{ for } h = 4
\end{aligned}$$

Step 4: Denote the OOC states as “**OOO**” given by Equation (A.1). For example, for $h = 3$, **OOO** = {AA, ABA, ABBA, CC, CBC, CBBC}.

Step 5: Combine the states in Step 2 to 4 to get the state space denoted by Ω . Therefore, the state space of the side-sensitive $SRR_{2-of-(h+1)}$ schemes are given by

$$\{\eta_1; \phi; \eta_3; \text{OOO}\} \text{ for } h = 1$$

$$\{\eta_1, \eta_2; \phi; \eta_4, \eta_5; \text{OOO}\} \text{ for } h = 2$$

(A.4)

$$\{\eta_1, \eta_2, \eta_3; \phi; \eta_5, \eta_6, \eta_7; \text{OOO}\} \text{ for } h = 3$$

$$\{\eta_1, \eta_2, \eta_3, \eta_4; \phi; \eta_6, \eta_7, \eta_8, \eta_9; \text{OOC}\} \text{ for } h = 4$$

Step 6: Construct the TPMs of the proposed KL schemes. For instance, when $h = 3$ the TPM of the side-sensitive $\text{SRR}_{2\text{-of-}(h+1)}$ scheme is constructed as follows:

Table A.2. Construction of the TPM of the side-sensitive $\text{SRR}_{2\text{-of-}(h+1)}$ scheme when $h = 3$

	η_1 {122}	η_2 {12}	η_3 {1}	ϕ {2}	η_5 {3}	η_6 {32}	η_7 {322}	OOC
$\eta_1=\{122\}$	0	0	0	p_2	p_3	0	0	p_1
$\eta_2=\{12\}$	p_2	0	0	0	p_3	0	0	p_1
$\eta_3=\{1\}$	0	p_2	0	0	p_3	0	0	p_1
$\phi=\{2\}$	0	0	p_1	p_2	p_3	0	0	0
$\eta_5=\{3\}$	0	0	p_1	0	0	p_2	0	p_3
$\eta_6=\{32\}$	0	0	p_1	0	0	0	p_2	p_3
$\eta_7=\{322\}$	0	0	p_1	p_2	0	0	0	p_3
OOC	0	0	0	0	0	0	0	1

Note that the side-sensitive $\text{IRR}_{2\text{-of-}(h+1)}$ and $\text{SRR}_{2\text{-of-}(h+1)}$ schemes are constructed in a similar way.